

Contents

Case 1: Pulmonary Alveolar Proteinosis	198
Case 2: Silicone Embolism	200
Case 3: Hypersensitivity Pneumonitis	202
Case 4: <i>P. jiroveci</i> Pneumonia	204
Case 5: Chronic Eosinophilic Pneumonia	206
Case 6: Pulmonary Langerhans Cell Histiocytosis.....	208
Case 7: Lymphocytic Interstitial Pneumonia	210
Case 8: Varicella Pneumonia.....	212
Case 9: Cryptogenic Organizing Pneumonia	214
Case 10: Lymphangioleiomyomatosis	216
Further Reading	218

Case 1: Pulmonary Alveolar Proteinosis

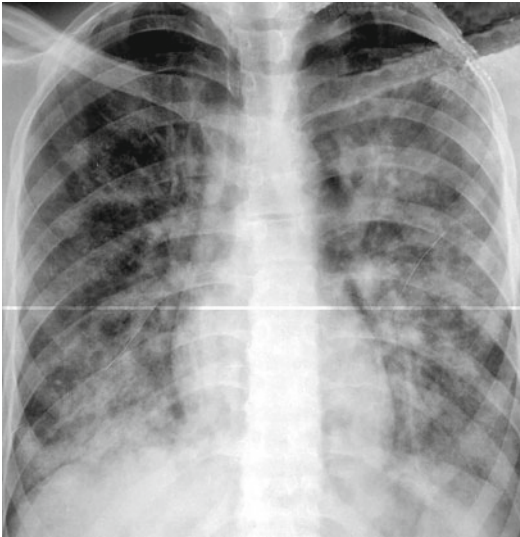


Fig. 9.1.1

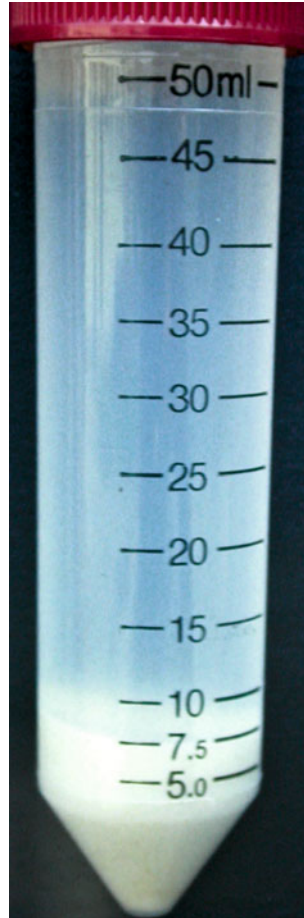


Fig. 9.1.4

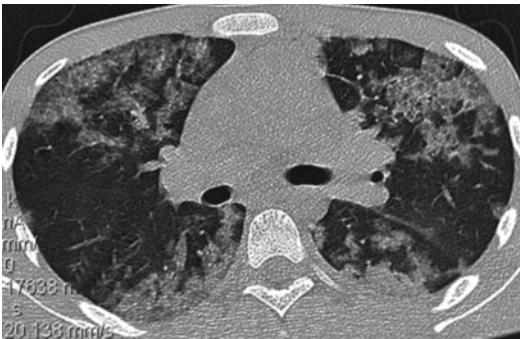


Fig. 9.1.2



Fig. 9.1.3

A 19-year-old patient with an 8-month history of dyspnea and productive cough with mucoid sputum. The diagnosis of pulmonary alveolar proteinosis was confirmed by bronchoalveolar lavage (BAL).

Pulmonary alveolar proteinosis (PAP) is an uncommon disease, characterized by alveolar accumulation of lipoproteinaceous material. PAP is classified in two main types: congenital and acquired. Congenital PAP (2 % of the cases) appears in the neonatal period as a clinical picture of acute respiratory distress. Acquired PAP is divided into idiopathic or autoimmune (90 % of the cases) and secondary, associated to exposure conditions (inhalation of silica, cotton, aluminum), infections (*P. asteroides*, cytomegalovirus), and immune disorders (human immunodeficiency virus infection, posttransplant immunosuppression).

PAP prevalence is 6.2 cases per million people, the disease is more prevalent in the male gender (3:1), and 39 years is the mean age at diagnosis.

The idiopathic or autoimmune type seems to be associated to the presence of antibodies against the granulocyte-macrophage colony-stimulating factor (GM-CSF), which alters the pulmonary surfactant metabolism.

Clinical features are nonspecific and the approximate average time between the onset of symptoms and the diagnosis is 7 months.

Radiological manifestations are diverse. The radiographic appearance most frequently described in the series consists of symmetrical central and basal consolidations. However, predominantly central reticular opacities, mixed opacities with reticulation and consolidation, and asymmetrical patchy parenchymal opacities may be found. In high-resolution computed tomography (HRCT), the most frequent finding is a “crazy paving” pattern (combination of ground-glass and linear opacities). Areas of “crazy paving” are typically bilateral, extensive, and follow a geographic pattern. Nevertheless, in some cases, the distribution can be asymmetrical, predominantly central, peripheral, or patchy. Other HRCT findings in patients with PAP include ground-glass opacities, consolidation, and airway irregularity.

CRX film shows multilobar consolidation (Fig. 9.1.1). HRCT shows crazy paving pattern with lower lobes predominance (Figs. 9.1.2 and 9.1.3). Gross photo of bronchoalveolar fluid shows the characteristic milky aspect (Fig. 9.1.4).

Comments

Imaging Findings

Case 2: Silicone Embolism

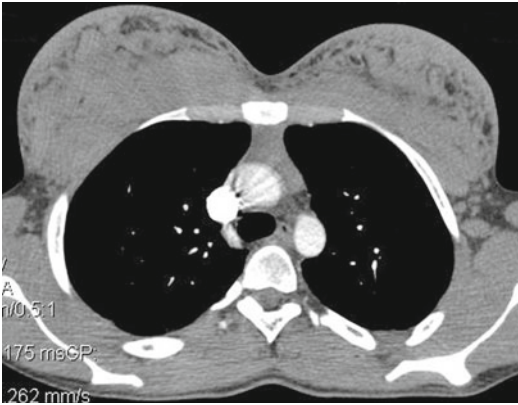


Fig. 9.2.1

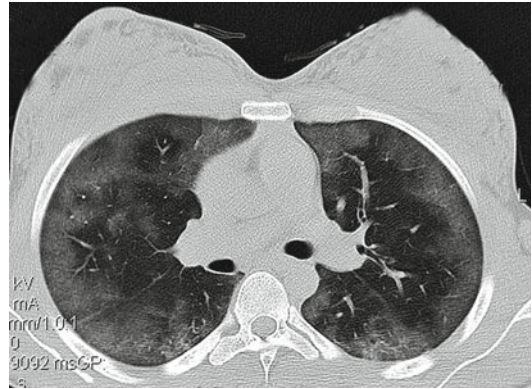


Fig. 9.2.2

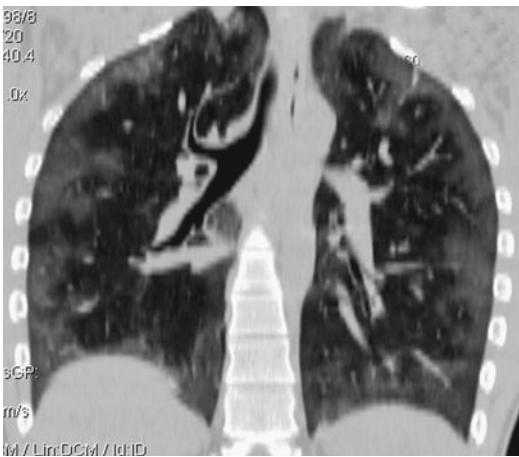


Fig. 9.2.3

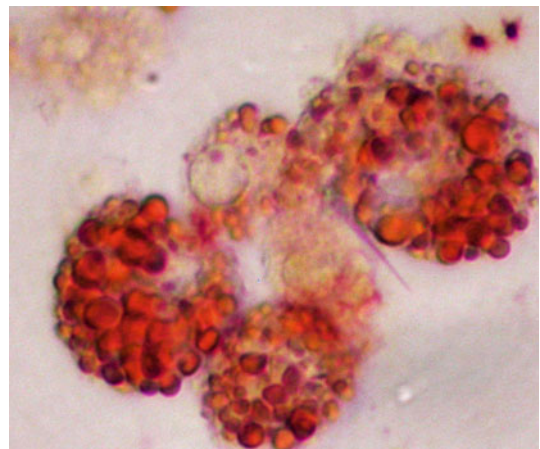


Fig. 9.2.4

A 24-year-old patient with a 24-h history of progressive dyspnea and dry cough, which started after an injection of liquid silicone in the pectoral region. The diagnosis of silicone pulmonary embolism was confirmed by the history, alterations in imaging studies, and the findings of a bronchoalveolar lavage (BAL).

Liquid silicone is a highly stable polymer, with minimum tissue reaction, widely used in the cosmetic industry. Subcutaneous injection of liquid silicone can be associated to pulmonary embolism. The preferred sites for subcutaneous injection of liquid silicone are the breasts and gluteus. Silicone pulmonary embolism (SPE) after a subcutaneous injection has been associated to the volume injected and to the local massages following the procedure.

The mechanism of pulmonary injury in these patients is similar to that described in fatty embolism with alveolar hemorrhage and fat globules in lung microcirculation and macrophages.

Sixty percent of the patients with SPE develop acute respiratory distress syndrome (ARDS), and 20 % die due to respiratory insufficiency.

All patients with SPE have abnormal chest x-rays with bilateral and peripheral ground-glass opacities, as the characteristic feature.

The most frequent HRCT abnormality in these patients is the presence of bilateral subpleural ground-glass opacities. Other findings in HRCT include thickening of interlobular septum and subpleural reticulation.

CT scan shows breast enlargement in male patient with increased density and nodular appearance of subcutaneous fat. Left axillary lymphadenopathy (Fig. 9.2.1). HRCT shows subpleural ground-glass opacity (Figs. 9.2.2 and 9.2.3). Bronchoalveolar lavage shows fat droplets and silicone within macrophages (Sudan stain, 40×; Fig. 9.2.4).

Comments

Imaging Findings

Case 3: Hypersensitivity Pneumonitis

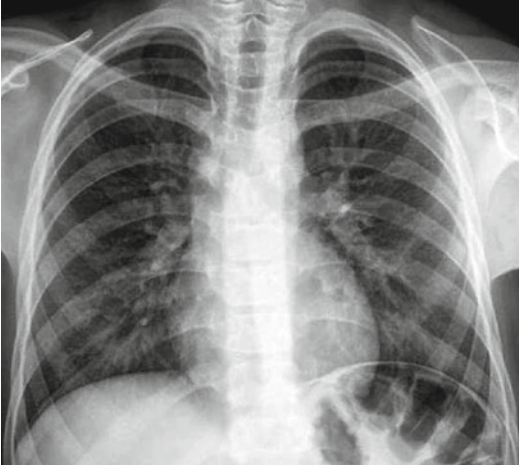


Fig. 9.3.1



Fig. 9.3.2

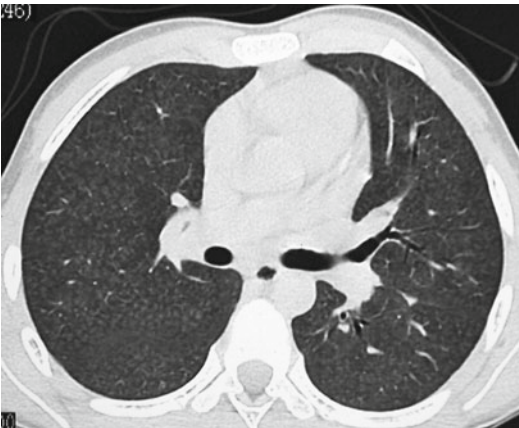


Fig. 9.3.3

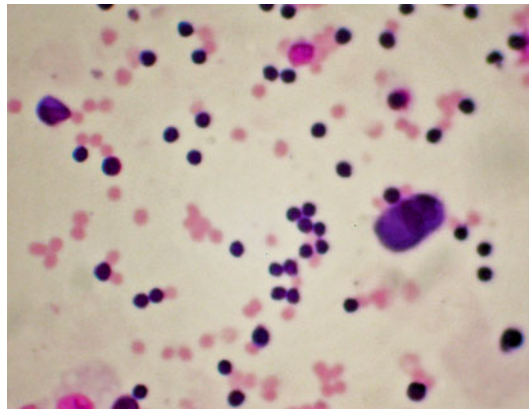


Fig. 9.3.4

A 16-year-old patient with repeated episodes of cough and dyspnea, which subsided spontaneously. There was a history of occasional contact with pigeons. The diagnosis of hypersensitivity pneumonitis was confirmed by the clinical findings, diagnostic images, and BAL findings.

Hypersensitivity pneumonitis (HN) is a pulmonary disease with symptoms of cough and dyspnea, produced by the inhalation of an allergen by a previously sensitized individual. Most antigens related with HN originate in bacteria (*Saccharopolyspora rectivirgula*), mold (*Penicillium* species), yeast, or poultry (pigeon proteins). Chemical agents such as isocyanates, zinc, tinctures, and dyes can act as haptens to induce HN.

In a study carried out in three European countries, HN represented between 4 and 15 % of pulmonary interstitial diseases.

HN has traditionally been classified in acute, subacute, and chronic. However, recent trials by the HN study group have had difficulties classifying patients in these groups and particularly in cases previously described as subacute.

In the acute phase, radiological abnormalities are similar to those described in pulmonary edema, with multilobar areas of consolidation. In the subacute phase, the main HRCT manifestations are: centrilobular nodule (ill defined), areas of ground-glass opacity (variable distribution and extension), and cystic lesions in 13 % of the cases. In the chronic phase, changes associated to pulmonary fibrosis are found, usually respecting lung bases, with reticular opacities, traction bronchiectasis, and limited areas of honeycombing.

CRX film shows diffuse micronodular opacities (Fig. 9.3.1). CT scan shows multiple ground-glass nodules with centrilobular distribution (Figs. 9.3.2 and 9.3.3). Bronchoalveolar lavage with lymphocyte proliferation (Diff-Quick stain, 10×; Fig. 9.3.4).

Comments

Imaging Findings

Case 4: *P. jiroveci* Pneumonia

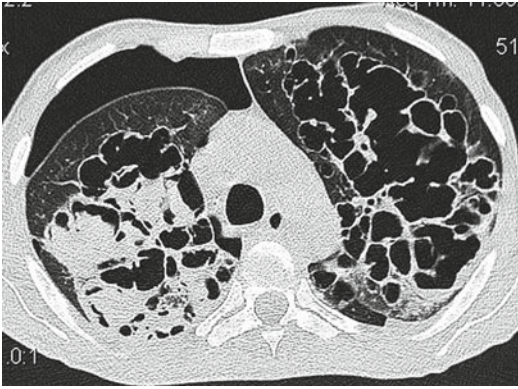


Fig. 9.4.1

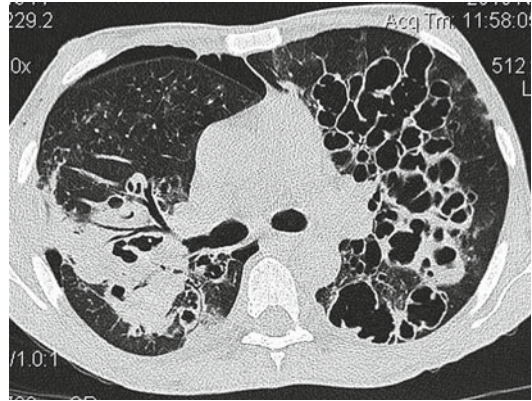


Fig. 9.4.2

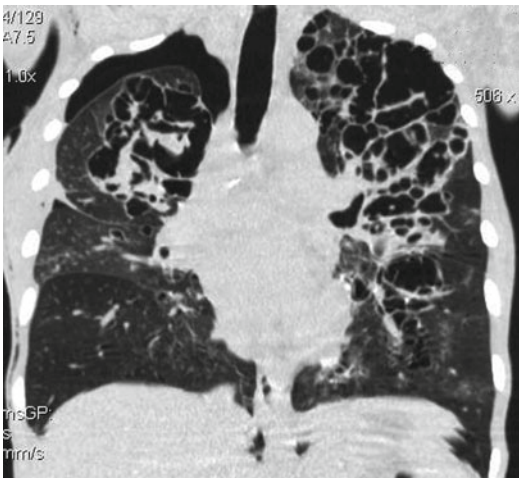


Fig. 9.4.3

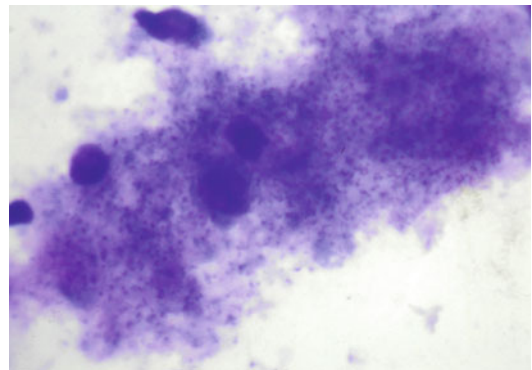


Fig. 9.4.4

A 23-year-old patient with acute chest pain (4 h before consulting the emergency room) and a 1-month history of dry cough and progressive dyspnea. The diagnosis of *P. jiroveci* pneumonia was confirmed by bronchoalveolar lavage.

P. jiroveci pneumonia (PJP) has been described in immunocompromised patients and particularly in patients with human immunodeficiency virus (HIV) infection. The current incidence of PCP in HIV (+) patients has decreased due to the use of high impact antiretroviral therapy and prophylaxis with trimethoprim/sulfamethoxazole. Nevertheless, PJP incidence remains high in HIV (+) patients in underdeveloped countries.

The clinical picture of PJP in HIV (+) patients is subacute and characterized by dry cough and progressive dyspnea (2–4 weeks).

Radiologic manifestations of *P. jiroveci* pneumonia include: predominantly central reticular opacities, ground-glass opacities, and mixed opacities. In HRCT, the predominant manifestation is the presence of ground-glass opacities with diverse distributions: central, in a “mosaic” pattern, or diffuse. As the infection progresses, areas of consolidation and reticular opacities may appear. The presence of cystic lesions in PJP is variable according to the series (10–20 % of patients). Cysts appear mainly in apical segments; have variable sizes, irregular margins, and thin or thick walls; and are associated with spontaneous pneumothorax.

HRCT shows thin-walled cystic appearance lesions without communication with airway. Peribronchial consolidation adjacent cystic lesions. Right pneumothorax. Upper lobes predominance of cystic appearance lesions (Figs. 9.4.1, 9.4.2, and 9.4.3). Bronchoalveolar fluid shows numerous trophozoites of pneumocystis (Diff-Quick stain, 40×; Fig. 9.4.4).

Comments

Imaging Findings

Case 5: Chronic Eosinophilic Pneumonia



Fig. 9.5.1

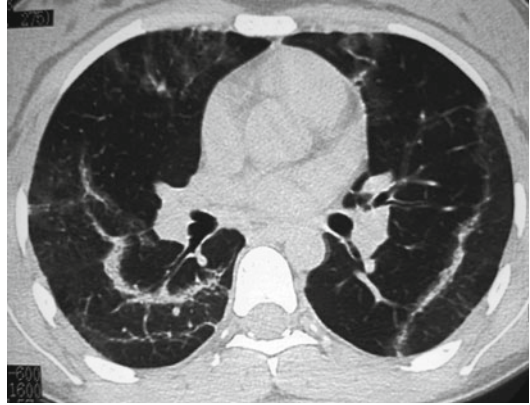


Fig. 9.5.3



Fig. 9.5.2

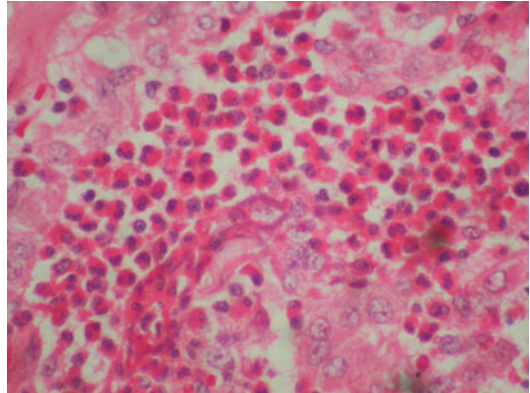


Fig. 9.5.4

A 32-year-old patient with a 6-month history of episodic productive cough with mucoid sputum and dyspnea. Eosinophilia was found in BAL and the diagnosis of chronic eosinophilic pneumonia was confirmed by open lung biopsy.

Chronic eosinophilic pneumonia (CEP) is an uncommon idiopathic disorder characterized by subacute or chronic respiratory and systemic symptoms, blood and/or alveolar eosinophilia, and peripheral opacities in the chest x-ray.

CEN is considered to represent between 0 and 2.5 % of pulmonary interstitial disease cases. This disorder is more frequent in women (2:1) and between one-third and half of the patients with CEP have a history of asthma.

Most CEP patients are symptomatic and the most frequent manifestations are: progressive dyspnea, cough, and general symptoms (asthenia, weight loss, and night sweats).

Eosinophilia is found in BAL (12–95 % of cellular count, with an average of 59 %). Lung biopsy shows evidence of predominantly eosinophilic alveolar and interstitial inflammatory infiltration.

The classic radiographic finding is the “inverse pulmonary edema” (peripheral, mainly apical, nonsegmental consolidation). However, this finding is seen in less than 50 % of the patients. HRCT manifestations are variable and related to disease evolution. Predominantly peripheral areas of ground-glass opacities and/or consolidation are more common in early stages. With disease progression, septal lines, reticular opacities, nodules, and subpleural parenchymal bands may be found.

CRX film shows multilobar and peripheral consolidation (Fig. 9.5.1; HRCT). Pulmonary architecture distortion. Parenchymal bands with traction bronchiectasis, ground-glass and subpleural consolidation (Figs. 9.5.2 and 9.5.3). Lung biopsy shows numerous eosinophils filling an alveolar space (HE, 40×; Fig. 9.5.4).

Comments

Imaging Findings

Case 6: Pulmonary Langerhans Cell Histiocytosis

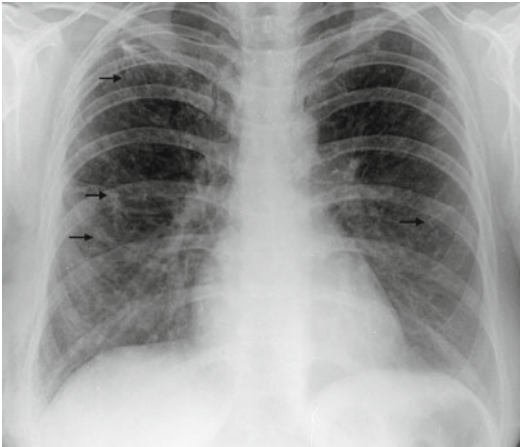


Fig. 9.6.1

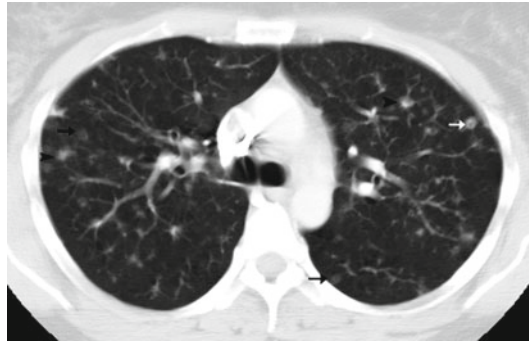


Fig. 9.6.2

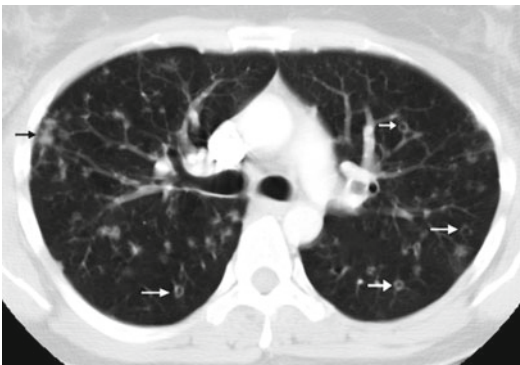


Fig. 9.6.3

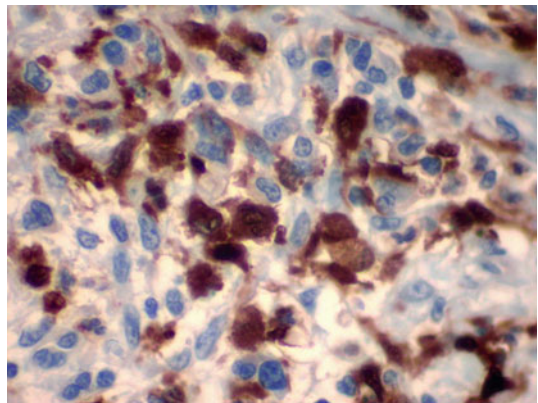


Fig. 9.6.4

A 40-year-old patient with progressive dyspnea starting 6 months before and a history of smoking. The diagnosis of Langerhans cell histiocytosis was made by an open lung biopsy.

Pulmonary Langerhans cell histiocytosis (PLCH) is an isolated form of Langerhans cell histiocytosis (LCH) that mainly affects smokers. Disease pathogenesis remains uncertain. LCH represents a clonal proliferation of cells similar to that typical of neoplastic diseases. In the particular case of the pulmonary type, pathogenesis may be different, as it has been demonstrated that most nodules do not follow clonal proliferation. It has been suggested that this disorder corresponds to an exaggerated immune response to an antigen, in which Langerhans cells can serve as accessory cells in T lymphocyte activation.

From the histological viewpoint, histiocytosis is a temporary heterogeneous disorder characterized by peribronchiolar proliferation of Langerhans cells, which form nodules. Nodular lesions frequently cavitate forming thick- or thin-walled cysts according to the evolutionary stage. These cysts represent the lumen of the dilated airway. In the most severe cases, the presence of fibrosis can reach the alveolar wall, forming scars and distorting pulmonary architecture.

It is a clinically rare disease (5 % of interstitial diseases). Patients are sometimes asymptomatic. However, the most frequent symptoms are cough and dyspnea. Other clinical manifestations can be hemoptysis, fever, weight loss, and night sweats. Pneumothorax, sometimes recurrent, can occur in one out of every four patients.

Radiological manifestations depend on the evolution of the disease.

Chest x-rays can be interpreted as normal in early stages of disease. In advanced cases, the most frequent semiological findings are reticular opacities corresponding to the visualization of the walls of contiguous cystic lesions and predominantly apical small nodules.

In HRCT, the most frequent manifestation of early disease is the presence of small, irregular, peribronchiolar nodules, with different degrees of cavitation in an otherwise healthy lung. With disease progression, cystic lesions increase in number and size and their walls become thinner. The presence of cystic lesions larger than 1 cm, with irregular margins, and distortion of pulmonary architecture suggests an advanced stage of the disease. Related findings include ground-glass opacities and changes due to emphysema associated to the habit of smoking.

CRX film shows ill-defined nodular opacities (arrows). Peribronchial thickening (Fig. 9.6.1).

CT scan shows ground-glass small nodules (black arrows) and soft tissue nodules (arrowheads), with varying degree of cavitation (white arrows) and random distribution (Figs. 9.6.2 and 9.6.3). Lung biopsy shows the typical nuclear and cytoplasmic staining of Langerhans cells (S-100 stain, 40×; Fig. 9.6.4).

Comments

Imaging Findings

Case 7: Lymphocytic Interstitial Pneumonia

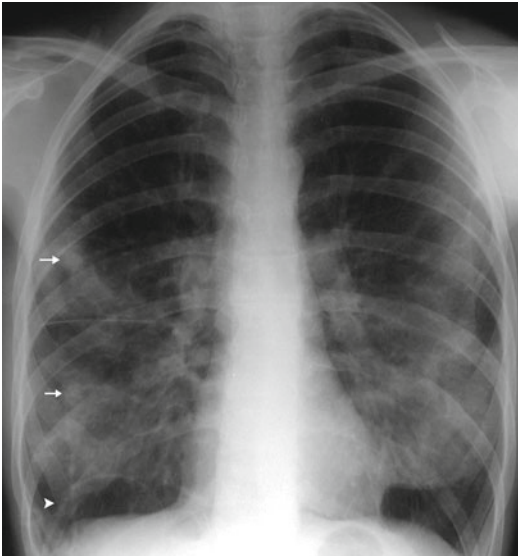


Fig. 9.7.1

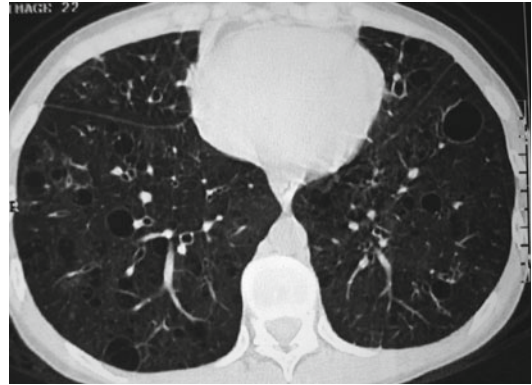


Fig. 9.7.2

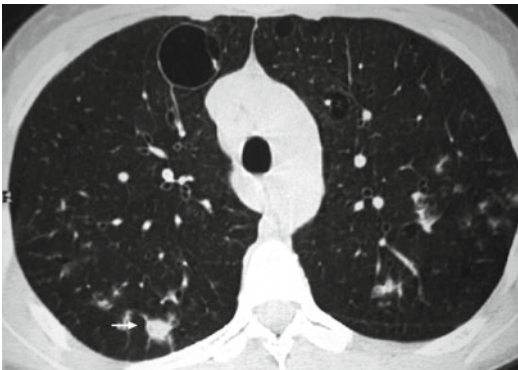


Fig. 9.7.3

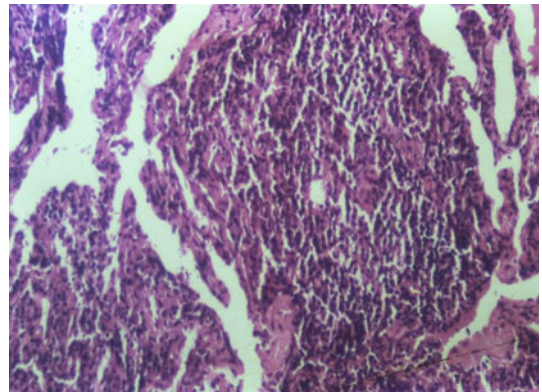


Fig. 9.7.4

A 43-year-old patient with a 1-year clinical picture consisting of cough and dyspnea and a 3-month history of weight loss and fever. After an open lung biopsy, the diagnosis of lymphocytic interstitial pneumonia was made.

Lymphocytic interstitial pneumonia (LIP) is considered a nonneoplastic inflammatory reaction of bronchial associated lymphoid tissue (BALT). This pattern of pulmonary response can be associated to systemic diseases (Sjögren syndrome, systemic lupus erythematosus), dysproteinemias, human immunodeficiency virus infection, and adverse reaction to drugs (diphenylhydantoin). In its idiopathic presentation, it is included in the group of idiopathic interstitial pneumonias, due to the presence of fibrosis during the course of the disease in some patients.

LIP may appear in pediatric population associated to HIV infection. Most adults with LIP are women between the 5th and 7th decades of life. Clinical manifestations are nonspecific and include cough and dyspnea of gradual onset. Less frequently, weight loss, chest pain, fever, and arthralgia are described.

Histologically, LIP is characterized by a lymphocitary infiltrate extensively compromising alveolar septa. Hyperplasia of type II pneumocytes and granuloma formation are described. Immunohistochemistry using CD20 shows that B cells are predominantly located in germ centers.

Radiological findings described in LIP are nonspecific, with predominantly basal reticular or reticulonodular opacities as the main manifestations. Areas of consolidation and ill-defined nodules may also be found. The most frequent alterations found in HRCT are ground-glass opacities, centrilobular nodules, thickening of peribronchovascular interstitium, interlobular septum thickening, areas of consolidation, and cysts. Pathogenesis of cysts is related to partial obstruction of bronchioles and air trapping due to peribronchial lymphocytic infiltration and occasionally due to focal amyloid deposits.

Chest x-ray film shows ill-defined nodules (arrow) and ground-glass patchy areas. Thin-walled cystic appearance lesion in right lower lobe (arrowhead) (Fig. 9.7.1). HRCT shows soft tissue nodules and diffuse ground-glass and thin-walled cystic lesions of variable size (Figs. 9.7.2 and 9.7.3). This photomicrograph shows the typical densely cellular appearance of widened alveolar septa (HE stain, 10×; Fig. 9.7.4).

Comments

Imaging Findings

Case 8: Varicella Pneumonia

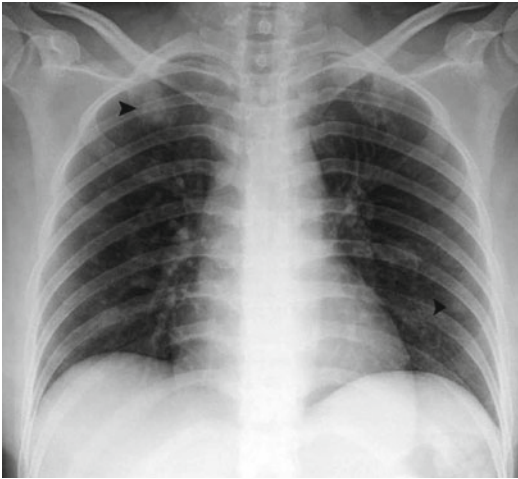


Fig. 9.8.1



Fig. 9.8.2

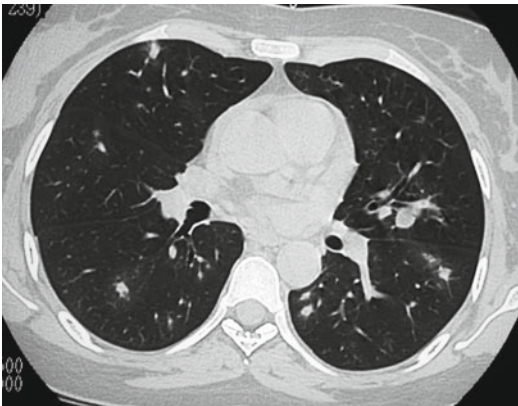


Fig. 9.8.3



Fig. 9.8.4

A 16-year-old patient with acute lymphocytic leukemia under treatment and a 6-day history of fever, dry cough, and cutaneous vesicular lesions. Considering the clinical picture and imaging study findings, the diagnosis of varicella pneumonia was made.

Pneumonia due to Varicella-Zoster virus is the most severe complication of a systemic infection, with a mortality rate ranging between 9 and 50 %.

Disease course in children is self-limited and benign. However, in adults, it tends to be a significant cause of complications. More than 90 % of cases of viral pneumonia due to Varicella-Zoster occur in immunocompromised adult patients and pregnant women.

There is no gender predilection. Conditions causing immunosuppression as leukemia, lymphoma, and corticosteroid therapy are considered risk factors. Pregnancy, advanced age, chronic obstructive pulmonary disease, and severe cutaneous eruption are other predisposing conditions.

Symptoms of pneumonia develop a few days after cutaneous vesicles appear and include cough, dyspnea, hemoptysis, tachypnea, pleuritic pain, and fever.

Histologically, they are nodules formed by areas of hyalinized collagen or necrotic tissue with a fibrous capsule that can resolve and calcify in various ways or form areas of mononuclear inflammatory interstitial infiltration with an intra-alveolar proteinaceous exudate and hyaline membrane formation (diffuse alveolar damage).

Radiological findings include ill-defined nodules, randomly distributed, ranging between 5 and 10 mm in diameter. Nodules can disappear or calcify late after cutaneous lesions have disappeared. Nodular lesions of soft tissue density, ranging between 1 and 10 mm in diameter, which may have a perilesional ground-glass halo, are described in HRCT. Nodular lesions can coalesce and combine with patchy ground-glass opacities.

Chest x-ray film shows nodular opacities, ill defined (arrowhead) (Fig. 9.8.1). Random soft tissue small nodules with ground-glass halo (Figs. 9.8.2 and 9.8.3). Vesicular lesions in the patient's forehead (Fig. 9.8.4).

Comments

Imaging Findings

Case 9: Cryptogenic Organizing Pneumonia

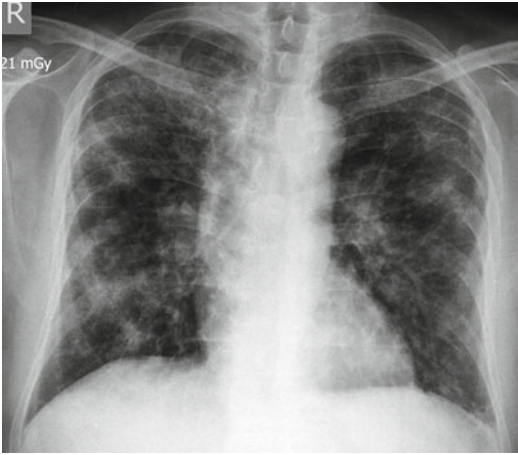


Fig. 9.9.1



Fig. 9.9.2

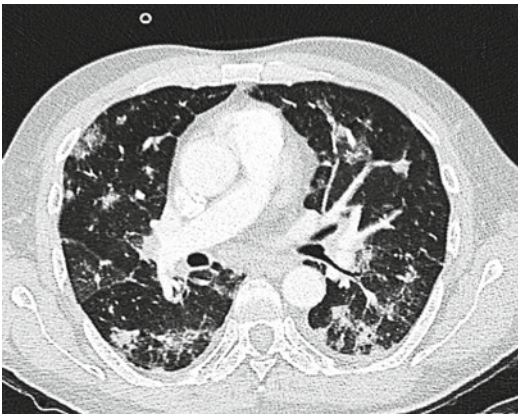


Fig. 9.9.3

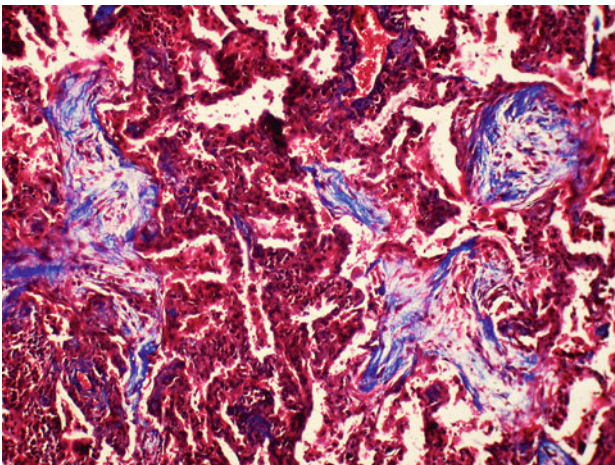


Fig. 9.9.4

A 39-year-old patient with a 3-month clinical picture consisting of fever, adynamia, weight loss, and cough. Open lung biopsy was interpreted as a pattern of organizing pneumonia. In the absence of an etiological factor or associated condition, the diagnosis of cryptogenic organizing pneumonia was made.

Organizing pneumonia (OP) is a nonspecific histopathological pattern of pulmonary response to injuries of diverse nature, characterized by the presence of granulation tissue buds in the distal airways. This process occurs mainly in alveoli, but may extend to alveolar duct lumen and bronchioles. OP can be classified in three categories: idiopathic (cryptogenic organizing pneumonia), of known cause (infection, radiation), or of unknown cause associated to a specific clinical context (collagen vascular disease, posttransplant).

The histological hallmark of organizing pneumonia is a distinct, usually patchy type of fibrosis that predominantly involves bronchiolar lumen and peribronchiolar airspaces. The fibrosis is composed of elongated fibroblasts and myofibroblasts arranged in parallel and embedded in a myxoid or pale staining matrix.

The typical or classical presentation of OP described in chest x-rays consists of bilateral patchy airspace consolidations, most prominent in the peripheral lower lung zones, with a tendency to progress and change location over time. CT reflects the findings of the chest x-ray demonstrating that the areas of consolidation are predominantly peribronchovascular and/or subpleural. Bronchial dilation in consolidated areas is described in 55 % of patients. Other findings in HRCT of patients with OP pattern are: nodule(s) – mass(es), ground-glass opacities, parenchymal bands, nodules with halo and reverse halo signs, and reticular opacities.

Chest x-ray film shows consolidation and ground-glass patchy (Fig. 9.9.1). CT scan (lung window) shows multilobar consolidation and ground-glass halo sign (Figs. 9.9.2 and 9.9.3). Lung biopsy shows fibroblast plugs within alveolar spaces (trichrome stain, 10×; Fig. 9.9.4).

Comments

Imaging Findings

Case 10: Lymphangioleiomyomatosis

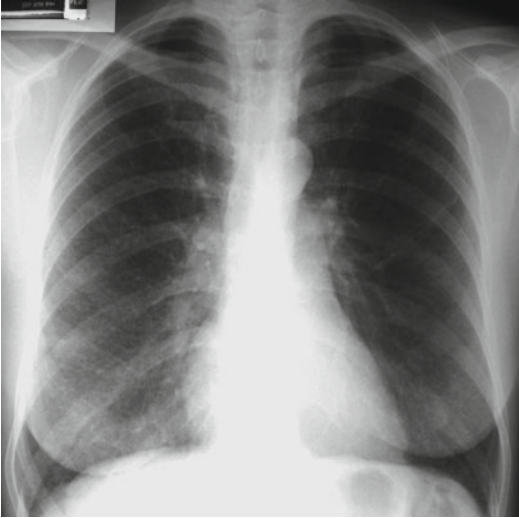


Fig. 9.10.1



Fig. 9.10.2

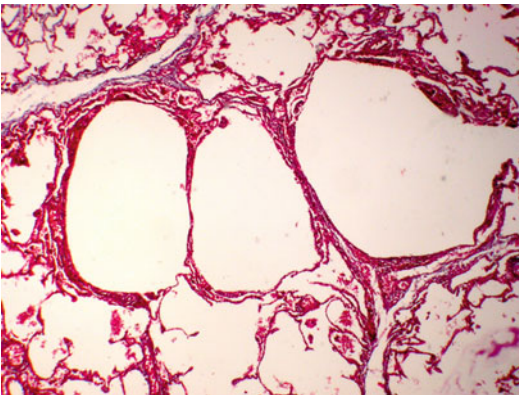


Fig. 9.10.3

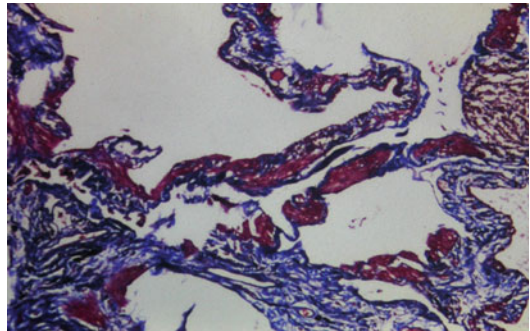


Fig. 9.10.4

A 28-year-old female patient with progressive dyspnea and a history of spontaneous pneumothorax. Open lung biopsy showed lymphangiomyomatosis.

Lymphangiomyomatosis (LLM) is a rare, progressive, multisystemic disorder characterized by the proliferation of pulmonary parenchyma bronchiolar, venular, and lymphatic smooth muscle. The pathogenesis is not clearly established but it probably has its bases in TSC2 gene mutations of the tuberous sclerosis complex located in chromosome 16.

Although classified as a different entity, LLM shares its physiopathology with tuberous sclerosis, and LLM patients may have extrapulmonary manifestations such as angiomyolipomas (15–30 % of patients). These similarities lead some researchers to consider LLM as a frustrated form of tuberous sclerosis or that both entities correspond to the same disease with a different degree of expression.

LLM affects almost exclusively women of childbearing age and can occur as a complication associated to tuberous sclerosis in women (men with tuberous sclerosis usually do not develop cystic changes of LLM in the lung).

Histologically, abnormal proliferation of immature smooth muscle cells within the airway, lymph vessels, and blood vessels causes mechanic obstruction with secondary cyst formation, pneumothorax, lymphatic flow obstruction, lymph node enlargement, chylothorax, and pulmonary arterial and venous hypertension that can lead to hemorrhage and hemothorax. A biochemical explanation for cyst formation in this disease is metalloprotease production by LAM cells, which destroy pulmonary collagen and elastin. LAM cells can be identified by immunohistochemistry techniques that demonstrate the presence of antigens to smooth muscle actin- and melanoma-associated HMB-45.

In chest x-rays, the most frequent manifestations are an increase in pulmonary volume and reticular opacities in relation to cyst overlapping.

HRCT shows multiple thin-walled cysts, of similar size and regular margins, uniformly distributed in lungs. Lung parenchyma in between cystic lesions is normal. These findings can simulate changes due to emphysema; the diagnostic key relies on the identification of cyst walls and the population group.

Chest x-ray film shows fine reticular opacities (Fig. 9.10.1). CT scan (lung window) shows diffuse and uniform small thin-walled cystic lesions (Fig. 9.10.2). Lung biopsy shows the characteristic smooth muscle in the cyst wall (HE and trichrome stain, 10×; Figs. 9.10.3 and 9.10.4).

Comments

Imaging Findings

Further Reading

Pulmonary Alveolar Proteinosis

- Borie RC et al (2011) Pulmonary alveolar proteinosis. *Eur Respir Rev* 20(120):98–107
- Godwin JD, Muller NL, Takasugi JE (1988) Pulmonary alveolar proteinosis: CT findings. *Radiology* 169:609–613
- Holbert JM et al (2001) CT features of pulmonary alveolar proteinosis. *AJR Am J Roentgenol* 176:1287–1294
- Johkoh T, Itoh H, Muller NL et al (1999) Crazy-paving appearance at thin-section CT: spectrum of disease and pathologic findings. *Radiology* 211:155–160
- Lee CH (2007) The crazy-paving sign. *Radiology* 243:905–906
- Muller NL, Fraser RS, Lee KS, Johkoh T (2003) Diseases of the lung: radiologic and pathologic correlations. Lippincott Williams & Wilkins, Philadelphia, pp 219–222
- Murrayama S, Murakami J, Yabuuchi H, Soeda H, Masuda K (1999) Crazy-paving appearance on high resolution CT in various diseases. *J Comput Assist Tomogr* 23:749–752
- Trapnell BC, Whitsett JA, Nakata K (2003) Pulmonary alveolar proteinosis. *N Engl J Med* 349:2527–2539

Silicone Embolism

- Bartsich S, Wu JK (2010) Silicon emboli syndrome: a sequela of clandestine liquid silicone injections. A case report and review of the literature. *J Plast Reconstr Aesthet Surg* 63:1–3
- Han D, Lee KS, Franquet T, Müller NL, Kim TS, Kim H et al (2003) Thrombotic and nonthrombotic pulmonary arterial embolism: spectrum of imaging findings. *Radiographics* 23:1521–1539
- Jorens PG, Van Marck E, Snoeckx A, Parizel PM (2009) Nonthrombotic pulmonary embolism. *Eur Respir J* 34:452–474
- Martínez JC, Manrique C, Sáenz O, Ojeda P, Nicolás Rocha N et al (2009) Silicone pulmonary embolism. Report of a case and review of the literature. *Rev Colomb Neumol* 21(2):84–88
- Price EA, Schueler H, Perper JA (2006) Massive systemic silicone embolism: a case report and review of literature. *Am J Forensic Med Pathol* 27:97–102
- Restrepo CS, Artunduaga M, Carrillo JA, Rivera AL, Ojeda P, Martínez-Jiménez S et al (2009) Silicone pulmonary embolism: report of 10 cases and review of the literature. *J Comput Assist Tomogr* 33:233–237
- Schmid A, Tzur A, Leshko L, Kriege BP (2005) Silicone embolism syndrome. *Chest* 127:2276–2281

Hypersensitivity Pneumonitis

- Glazer CS, Rose CS, Lynch DA (2002) Clinical and radiologic manifestations of hypersensitivity pneumonitis. *J Thorac Imaging* 17:261–272
- Hanak V, Golbin JM, Hartman TE et al (2008) High-resolution CT findings of parenchymal fibrosis

correlate with prognosis in hypersensitivity pneumonitis. *Chest* 134:133–138

- Hansell DM, Wells AU, Padley SP et al (1996) Hypersensitivity pneumonitis: correlation of individual CT patterns with functional abnormalities. *Radiology* 199:123–128
- Hirschmann JV, Pipavath SN, Godwin JD (2009) Hypersensitivity pneumonitis: a historical, clinical, and radiologic review. *Radiographics* 29:1921–1938
- Lynch DA, Rose CS, Way D et al (1992) Hypersensitivity pneumonitis: sensitivity of high-resolution CT in a population-based study. *Am J Roentgenol* 159:469–472
- Lynch DA, Newell JD, Logan PM et al (1995) Can CT distinguish hypersensitivity pneumonitis from idiopathic pulmonary fibrosis? *Am J Roentgenol* 165:807–811
- Ranks TJ, Galvin JR, Frazier AA (2004) The impact and use of high-resolution computed tomography in diffuse lung disease. *Curr Diagn Pathol* 10:279–290
- Silva CI, Churg A, Müller NL (2007) Hypersensitivity pneumonitis: spectrum of high-resolution CT and pathologic findings. *AJR Am J Roentgenol* 188:334–344
- Silva CI, Muller NL, Lynch DA et al (2008) Chronic hypersensitivity pneumonitis: differentiation from idiopathic pulmonary fibrosis and nonspecific interstitial pneumonia by using thin-section CT. *Radiology* 246:288–297

P. jiroveci Pneumonia

- Boiselle PM, Crans CA, Kaplan MA (1999) The changing face of *Pneumocystis carinii* pneumonia in AIDS patients. *AJR Am J Roentgenol* 172(5):1301–1309
- Hartman TE, Primack SL, Müller NL et al (1994) Diagnosis of thoracic complications in AIDS: accuracy of CT. *AJR Am J Roentgenol* 162(3):547–553
- Hidalgo A, Falcó V, Mauleón S et al (2003) Accuracy of high-resolution CT in distinguishing between *Pneumocystis carinii* pneumonia and non-*Pneumocystis carinii* pneumonia in AIDS patients. *Eur Radiol* 13(5):1179–1184
- Kanne JP, Yandow DR, Meyer CA (2012) *Pneumocystis jiroveci* pneumonia: high-resolution CT findings in patients with and without HIV infection. *AJR Am J Roentgenol* 198:W555–W561
- Opravil M, Marincek B, Fuchs WA et al (1994) Shortcomings of chest radiography in detecting *Pneumocystis carinii* pneumonia. *J Acquir Immune Defic Syndr* 7(1):39–45
- Shah RM, Kaji AV, Ostrum BJ et al (1997) Interpretation of chest radiographs in AIDS patients: usefulness of CD4 lymphocyte counts. *Radiographics* 17(1):47–58

Chronic Eosinophilic Pneumonia

- Ebara H, Ikezoe J, Johkoh T, Kohno N, Takeuchi N, Kozuka T et al (1994) Chronic eosinophilic pneumonia: evolution of chest radiograms and CT features. *J Comput Assist Tomogr* 18(5):737–744

- Gaenster EA, Carrington B (1977) Peripheral opacities in chronic eosinophilic pneumonia: the photographic negative of pulmonary edema. *AJR Am J Roentgenol* 128:1-13
- Jeong YJ et al (2007) Eosinophilic lung diseases: a clinical, radiologic, and pathologic overview. *Radiographics* 27:617-639
- Johkoh T, Müller NL, Akira M et al (2000) Eosinophilic lung diseases: diagnostic accuracy of thin-section CT in 111 patients. *Radiology* 216(3):773-780
- Mayo JR, Muller NL, Sisler J, Lillington G (1989) Chronic eosinophilic pneumonia: CT findings in six cases. *AJR Am J Roentgenol* 153:727-730

Pulmonary Langerhans Cell Histiocytosis

- Abbott GF, Rosado-de-Christenson ML et al (2004) Pulmonary Langerhans cell histiocytosis. *Radiographics* 24:821-841
- Brauner MW, Grenier P, Tijani K et al (1997) Pulmonary Langerhans cell histiocytosis: evolution of lesions on CT scans. *Radiology* 204(2):497-502
- Ko S-M et al (2008) Atypical radiological manifestations of pulmonary Langerhans cell histiocytosis in a 12-year-old girl. *Br J Radiol* 81:e238-e241
- Leatherwood DL, Heitkamp DE, Emerson RE (2007) Pulmonary Langerhans cell histiocytosis. *Radiographics* 27:265-268
- Moore AD, Godwin JD, Müller NL et al (1989) Pulmonary histiocytosis X: comparison of radiographic and CT findings. *Radiology* 172(1):249-254
- Schmidt S, Eich G, Geoffroy A et al (2008) Extraosseous Langerhans cell histiocytosis in children. *Radiographics* 28(3):707-726
- Suri H et al (2012) Pulmonary Langerhans cell histiocytosis. *Orphanet J Rare Dis* 7:16
- Tazi A (2006) Adult pulmonary Langerhans' cell histiocytosis. *Eur Respir J* 27:1272-1285
- Tazi A, Soler P, Hance AJ (2000) Adult pulmonary Langerhans' cell histiocytosis. *Thorax* 55:405-416

Lymphocytic Interstitial Pneumonia

- Honda O, Johkoh T, Ichikado K et al (1999) Differential diagnosis of lymphocytic interstitial pneumonia and malignant lymphoma on high-resolution CT. *AJR Am J Roentgenol* 173(1):71-74
- Johkoh T, Muller NL et al (1999) Lymphocytic interstitial pneumonia: thin-section CT findings in 22 patients. *Radiology* 212:567-572
- Kim TS, Lee KS, Chung MP et al (1998) Nonspecific interstitial pneumonia with fibrosis: high-resolution CT and pathologic findings. *AJR Am J Roentgenol* 171(6):1645-1650

- Swigris JJ, Berry GJ, Raffin TA, Kuschner WG (2002) Lymphoid interstitial pneumonia: a narrative review. *Chest* 122(6):2150-2164

Varicella Pneumonia

- Aquino SL, Dunagan DP, Chiles C, Haponik EF (1998) Herpes simplex virus I pneumoniae patterns on CT scans and conventional chest radiographs. *J Comput Assist Tomogr* 22:795-800
- Franquet T (2011) Imaging of pulmonary viral pneumonia. *Radiology* 260:18-39
- Kim EA et al (2002) Viral pneumonias in adults: radiologic and pathologic findings. *Radiographics* 22:S137-S149
- Maher TM et al (2007) CT findings of varicella pneumonia after lung transplantation. *AJR Am J Roentgenol* 188:W557-W559
- Umans U, Golding RP, Duraku S, Manoliu RA (2001) Herpes simplex virus I pneumonia: conventional chest radiograph pattern. *Eur Radiol* 11:990-994

Cryptogenic Organizing Pneumonia

- Cordier JF (2000) Organising pneumonia. *Thorax* 55:318-328
- Greenberg-Wolff I et al (2005) Cryptogenic organizing pneumonia: variety of radiologic findings. *Isr Med Assoc J* 7:568-570
- King TE Jr, Mortenson RL (1992) Cryptogenic organizing pneumonitis. The North American Experience. *Chest* 102:8S-13S
- Lee KS, Kullnig P, Hartman TE, Muller NL (1994) Cryptogenic organizing pneumonia: CT findings in 43 patients. *Am J Roentgenol* 162:543-546
- Thurlbeck WM, Miller RR, Muller NL, Rosenow ECI (1991) Diffuse diseases of the lung: a team approach. BC Decker, Philadelphia
- Ujita M et al (2004) Organizing pneumonia: peribubular pattern at thin-section CT. *Radiology* 232:757-761

Lymphangioliomyomatosis

- Abbott GF, Rosado-de-Christenson ML, Frazier AA, Franks TJ, Pugatch RD, Galvin JR (2005) Lymphangioliomyomatosis: radiologic-pathologic correlation. *Radiographics* 25:803-828
- Avila NA, Dwyer AJ, Moss J (2011) Imaging features of lymphangioliomyomatosis: diagnostic pitfalls. *AJR Am J Roentgenol* 196:982-986
- Johnson SR, Cordier JF et al (2010) European Respiratory Society guidelines for the diagnosis and management of lymphangioliomyomatosis. *Eur Respir J* 35:14-26
- Lim KE et al (2004) Pulmonary lymphangioliomyomatosis high-resolution CT findings in 11 patients and compared with the literature. *J Clin Imaging* 28:1-5